Millimeter-wave FET modeling using on-wafer measurements and EM simulation

(Article begins on next page)

Millimeter-Wave FET Modeling Using On-Wafer Measurements and EM Simulation

Alessandro Cidronali, *Member, IEEE*, Giovanni Collodi, *Member, IEEE*, Alberto Santarelli, *Member, IEEE*, Giorgio Vannini, *Member, IEEE*, and Gianfranco Manes, *Member, IEEE*

Abstract—Electron device modeling is a challenging task at millimeter-wave frequencies. In particular, conventional approaches based on lumped equivalent circuits become inappropriate to describe complex distributed and coupling effects, which may strongly affect the transistor performance. In this paper, an empirical distributed FET model is adopted that can be identified on the basis of conventional S-parameter measurements and electromagnetic simulations of the device layout. The consistency of the proposed approach is confirmed by robust scaling properties, which enable millimeter-wave small-signal S-parameters to be predicted as a function of the device periphery and number of gate fingers. Moreover, it is shown how the model identified on the basis of standard S-parameter measurements up to 50 GHz can be efficiently exploited in order to obtain reasonably accurate small-signal prediction up to 110 GHz. Extensive experimental validation is presented for 0.2-μm pseudomorphic high electron-mobility transistors devices.

Index Terms—Computer-aided engineering, electromagnetic simulation, global modeling, millimeter-wave FETs, MODFET, semiconductor device modeling.

I. INTRODUCTION

INCREASING operating frequencies in many applications of the communication area require accurate computer-aided design (CAD) tools for monolithic-microwave integrated-circuit (MMIC) design in order to face off demanding low-cost constraints [1]. In this context, accurate electron device models up to millimeter-wave frequencies play a key role; in spite of this, conventional modeling approaches, based on lumped equivalent circuits, become inappropriate at very high frequencies where complex distributed and coupling effects strongly affect the transistor performance [2], [3].

Over the last years, a progress in numerical device simulation and the development of electromagnetic analysis tools [4]–[6], together with the availability of powerful workstations, have led to modeling approaches aiming to a consistent numerical solution of the electromagnetic and electron transport problems. Although these models are potentially accurate, they are still in a preliminary phase and their application to practical problems such as circuit analysis, design, and optimization may be difficult, also taking into account their computational cost [7]–[12]. On the other hand, there is an increasing demand for comprehensive and effective analysis/design tools able to consider simultaneously (i.e., "*global modeling*" [13]–[20]) all the interacting circuit elements, active and passive devices, radiation elements, and packaging influence.

A circuit-design-oriented family of distributed models for electron devices has recently appeared in the literature. They are based on the common idea of an extrinsic passive network feeding a cascade of elementary active devices [20]–[28]. In comparison with other approaches, the empirical model presented in [20] adopts a distributed description both for the active device area and extrinsic structure. In particular, according to this FET modeling approach, the active area is partitioned into a convenient number of "*internal elementary devices*" (or "*active slices*") fed by a "*passive distributed structure*." This one is characterized in terms of scattering parameters by means of an accurate electromagnetic simulation of the device layout. This kind of analysis enables the actual device geometry and material stratification, as well as losses in the dielectrics and metallizations, to be taken into account for any given device structure and size by means of a multiport S-matrix distributed description. Therefore, on the basis of S-parameters measured for a limited number of different devices, a characterization of the intrinsic slices associated with the active phenomena can be easily obtained.

In [20], the empirical distributed model was adopted in order to predict, as a function of the device periphery and number of gate fingers, small-signal S-parameters (up to 50 GHz) for GaAs MESFETs. In particular, preliminary experimental results have confirmed the consistency of the model pointing out useful robust scaling properties, which enable transistor geometric parameters to be considered as circuit design variables. In this paper, an extensive and more significative validation of the model up to very high frequencies (110 GHz) is presented for 0.2-μm pseudomorphic high electron-mobility transistor (pHEMT) devices. Besides scaling results, a new frequency extrapolation approach, suitable for small-signal performance prediction at frequencies much higher than those considered in model identification, is also presented. More precisely, it is shown how small-signal S-parameters can be predicted with reasonable accuracy up to 110 GHz using a model identified only on the basis of 50-GHz measurements. This, besides confirming the consistency and accuracy of the proposed empirical model, enable millimeter-wave device
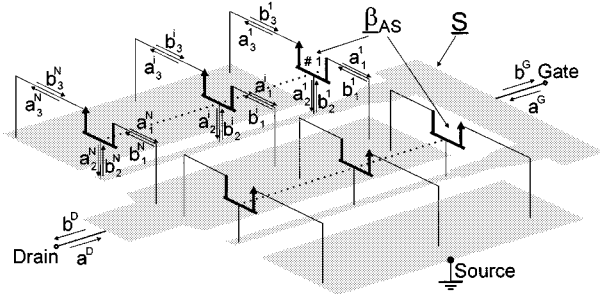
Fig. 1.   Structure of the distributed model.

characterization to be performed on the basis of "relatively standard" (50 GHz) network analyzers.

The paper is organized as follows. In Section II, the empirical distributed model and its identification procedure are shortly recalled. In Section III, considerations on the number of active slices required in the distributed model for millimeter-wave applications are provided. Finally, Section IV describes the frequency extrapolation approach proposed. Experimental results for several Philips 0.2-μm pHEMT structures, differing in terms of gatewidth and number of gate fingers, are provided both for scaling properties and frequency extrapolation in Sections III and IV, respectively.

II. EMPIRICAL DISTRIBUTED MODEL

The schematic structure of the model is shown in Fig. 1, where, for simplicity and without loss of generality, a two-finger device has been considered. In particular, the model consists of a "passive distributed network" to which $2N$ "active slices" are interconnected [20]. The passive structure is characterized by means of its scattering matrix $\underline{\mathbf{S}}$, which is computed by using electromagnetic simulation on the basis of layout geometry and material parameters. The matrix $\underline{\mathbf{S}}$, according to Fig. 1, relates the reflected waves to the incident ones as

$$[b^G \quad b^D \quad \mathbf{b^1} \quad \cdots \quad \mathbf{b^i} \quad \cdots \quad \mathbf{b^{2N}}]^T$$
$$= \underline{\mathbf{S}} \cdot [a^G \quad a^D \quad \mathbf{a^1} \quad \cdots \quad \mathbf{a^i} \quad \cdots \quad \mathbf{a^{2N}}]^T \quad (1)$$

where $\mathbf{a^i}$ and $\mathbf{b^i}$ are three-dimensional vectors of the incident and reflected waves at the interconnection with the ith active slice.

Basically, model identification may be seen as a deembedding procedure leading to the evaluation of the scattering matrices associated with the active slices starting from the knowledge of measured S-parameters of the electron device; in particular, the important assumption[1] is made that all the active slices are characterized by the same three-port scattering matrix $\underline{\beta}_{\mathbf{AS}}$, being $\mathbf{a^i} = \underline{\beta}_{\mathbf{AS}} \cdot \mathbf{b^i}$ according to Fig. 1.

By denoting with $\underline{\tilde{\mathbf{S}}}$ the scattering matrix obtained from $\underline{\mathbf{S}}$, once the rows and columns that are linearly dependent due to the symmetry of the device structure[2] have been eliminated, it can

[1]This assumption is quite reasonable since all the electromagnetic effects associated with signal propagation and distribution are accounted for by the passive structure.

[2]A symmetric structure is very common in all high-frequency devices.

be shown that the following homogeneous system of equations can be written:

$$\left[\begin{bmatrix} \underline{\mathbf{n}}_{1,1} & \underline{\mathbf{n}}_{1,2} & \vdots & \underline{\mathbf{n}}_{1,N} \\ \underline{\mathbf{n}}_{2,1} & \underline{\mathbf{n}}_{2,2} & \vdots & \underline{\mathbf{n}}_{2,N} \\ \cdots & \cdots & \ddots & \cdots \\ \underline{\mathbf{n}}_{N,1} & \underline{\mathbf{n}}_{N,2} & \vdots & \underline{\mathbf{n}}_{N,N} \end{bmatrix}\right.$$
$$\left. - \begin{bmatrix} \underline{\beta}_{\mathbf{AS}} & 0 & \cdots & 0 \\ 0 & \underline{\beta}_{\mathbf{AS}} & \cdots & 0 \\ \vdots & \vdots & \ddots & \vdots \\ 0 & 0 & \cdots & \underline{\beta}_{\mathbf{AS}} \end{bmatrix}\right] \cdot \begin{bmatrix} \mathbf{b^1} \\ \mathbf{b^2} \\ \vdots \\ \mathbf{b^{N-1}} \\ \mathbf{b^N} \end{bmatrix} = \underline{\mathbf{0}} \quad (2)$$

where N is the number of active slices included within each "half device."

In (2), the generic element having position p, q within the matrices $\underline{\mathbf{n}}_{\mathbf{h,k}}$ is defined as

$$\left(\underline{\mathbf{n}}_{\mathbf{h,k}}\right)_{p,q} = \left(\left[\underline{\sigma} \cdot \left[\frac{[\underline{\alpha} - \underline{\delta}]^{-1} \cdot \underline{\gamma}}{\underline{\mathbf{I}}}\right]\right]^{-1}\right)_{3h-3+p,\, 3k-3+q},$$
$$h, k = 1, \ldots, N; \quad p, q = 1, 2, 3 \quad (3)$$

with

$$\underline{\sigma}_{i=1,\ldots,3N;\, j=1,\ldots,2+3N} = \underline{\tilde{\mathbf{S}}}_{i=3,\ldots,2+3N;\, j=1,\ldots,2+3N}$$
$$\underline{\delta}_{i=1,2;\, j=1,2} = \underline{\tilde{\mathbf{S}}}_{i=1,2;\, j=1,2}$$
$$\underline{\gamma}_{i=1,2;\, j=1,\ldots,3N} = \underline{\tilde{\mathbf{S}}}_{i=1,2;\, j=3,\ldots,2+3N} \quad (4)$$

$\underline{\alpha}$ being the measured 2×2 scattering matrix of the electron device and $\underline{\mathbf{I}}$ being a $3N \times 3N$ identity matrix.

The unknown quantities in (2) are represented by the active slice matrix $\underline{\beta}_{\mathbf{AS}}$ and the vectors $\mathbf{b^i}$. Since we are concerned with the computation of $\underline{\beta}_{\mathbf{AS}}$, the waves $\mathbf{b^i}$ can be eliminated by proper algebraic manipulations. In the general case, this results in a nonlinear system of equations whose complexity depends on the number N of active slices. In the most simple case of $N = 1$, performing matrix arrangements, the solution of (2) leads to

$$\underline{\beta}_{\mathbf{AS}} = \left[\underline{\sigma} \cdot \left[\frac{[\underline{\alpha} - \underline{\delta}]^{-1} \cdot \underline{\gamma}}{\underline{\mathbf{I}}}\right]\right]^{-1}. \quad (5)$$

The formulation of the problems for the case $N = 2, 3$, and 4 is more cumbersome and is given in the Appendix.

It must be pointed out that, in any case, model identification (i.e., the computation of $\underline{\beta}_{\mathbf{AS}}$) does not require either optimization or parameter fitting.

The validity of the approach above described is confirmed by the consistency of the distributed model with a simple linear scaling rule. In particular, as experimentally verified in [20], the

TABLE I
MAGNITUDE OF THE SCALING FUNCTIONS $\hat{Y}_{21}$ AND $C_{21} \cdot K$ VERSUS FREQUENCY AND ACTIVE SLICE NUMBER PER FINGER FOR TWO-FINGER PML pHEMTs BIASED AT $V_{\mathrm{DS}} = 3$ V AND $I_D = I_{\mathrm{DSS}}$

Freq [GHz]	K=1		K=2		K=4	
	$\hat{Y}_{21}$ [mS/μm]	$C_{21} \cdot N$ [mS]	$\hat{Y}_{21}$ [mS/μm]	$C_{21} \cdot N$ [mS]	$\hat{Y}_{21}$ [S/μm]	$C_{21} \cdot N$ [mS]
2	0.439	0.390	0.438	0.401	0.438	0.406
10	0.346	2.610	0.348	2.594	0.348	2.602
30	0.113	6.194	0.125	6.060	0.127	6.057
50	0.032	6.679	0.043	6.558	0.046	6.545
70	0.008	5.654	0.011	5.628	0.012	5.637
90	-0.002	4.527	-0.001	4.665	-0.001	4.729
110	0.013	1.991	0.098	2.528	0.004	2.697

admittance[3] matrix of the elementary device can be properly scaled according to the following rule:

$$\underline{\mathbf{Y}}_{\mathbf{AS}}(\omega, W_{AS}) = \hat{\underline{\mathbf{Y}}}(\omega) \cdot W_{AS} + \underline{\mathbf{C}}(\omega) \quad (6)$$

where W_{AS} is the active slice width and $\hat{\underline{\mathbf{Y}}}$, $\underline{\mathbf{C}}$ are suitable width-independent "scaling functions." More precisely, $\hat{\underline{\mathbf{Y}}}(\omega)$ is an admittance matrix per unit of gatewidth, while $\underline{\mathbf{C}}(\omega)$ represents a fraction of the active slice admittance matrix, which accounts for nonideal border-like effects due to the actual device geometry [20]. Once the functions $\hat{\underline{\mathbf{Y}}}(\omega)$ and $\underline{\mathbf{C}}(\omega)$ have been evaluated, on the basis of the admittance matrix $\underline{\mathbf{Y}}_{\mathbf{AS}}$ identified for at least two devices having different gatewidths, the linear rule (6) can be used to obtain the equivalent admittance matrix associated with an active slice as a function of its width. The characterization obtained in this way for the active slice in conjunction with electromagnetic simulation of the device layout was successfully used in [20] to predict small-signal scattering parameters up to 50 GHz for MESFET devices having different geometries.

III. MILLIMETER-WAVE FET MODELING

Numerical analysis of the signal propagation along the microwave FET electrodes (see, for example, [9]), shows that three fundamental propagation modes are supported. They are governed both by the dielectric/metallization characteristics and by the "active" behavior of the semiconductor beneath the gate; in particular, conditions of slow-wave-like properties [9] can be found. Cases of study demonstrate possible values of the phase constant around 10^3 m^{-1} and attenuation constant around 50 dB/mm at 100 GHz, for $gm = 100$ mS/mm. For those values, the gatewidth of practical FET structures can be considered short with respect to the wavelength (i.e., $<\lambda/10$) suggesting that a model structure based on just one active slice per device finger should be reasonable for performance prediction up to relatively high frequencies.

The above considerations are coherent with the experimental results presented in [20], where a distributed model based on a single active slice per finger has been successfully adopted for the prediction of small-signal S-parameters of different MESFET structures in the microwave frequency range up to 50 GHz. However, in state-of-the-art pHEMTs, geometries, materials, and electric characteristics are strongly different

from those considered in [9] and similar numerical analyses of the signal propagation properties are not available in the literature. Consequently, in the perspective of millimeter-wave device modeling up to frequencies on the order of 100 GHz and more, it is worth wondering whether a single active slice per finger still allows for accurate performance prediction. To this aim, the model identification process described above has been repeated varying the number of active slices per finger and comparing the corresponding scaling functions.

In particular, different structures of Philips 0.2-μm GaAs pHEMT devices were considered to validate the modeling approach. More precisely, the scattering matrices of the extrinsic passive structures were computed using the planar three-dimensional (3-D) "*em*" Sonnet electromagnetic simulator[4] and the scattering parameters of the electron devices were measured directly on-wafer up to a frequency of 110 GHz. The matrices $\hat{\underline{\mathbf{Y}}}^{\mathbf{K}}(\omega)$ and $\underline{\mathbf{C}}^{\mathbf{K}}(\omega)$ in (6) were evaluated for a number K of active slices per finger ranging from 1 to 4, on the basis of a linear regression applied to a set of device structures covering a wide range of gatewidths instead of using the minimum set of two different devices. In particular, model identification was carried out using four different pHEMT structures, namely, 2 × 15 μm, 2 × 30 μm, 2 × 60 μm, and 2 × 120 μm. If an insufficient number of active slices per gate finger were considered in this phase, part of the parasitic effects, taken into account by the electromagnetic simulation of the device metallizations, could affect the extracted active slice models $\underline{\beta}_{\mathbf{AS}}$ (or, similarly, $\underline{\mathbf{Y}}_{\mathbf{AS}}$). In such conditions, the linear scaling rule (6), which is physically consistent only with the active area of the device, should have a very limited accuracy.

In Table I, the magnitude of the per-unit-gatewidth $\hat{Y}_{21}$ and $C_{21} \cdot K$ parameters[5] are reported for some frequency values up to 110 GHz and for different values of K. As can be seen, the scaling elements do not seem to exhibit significant variations versus the K values, apart from small deviations at the highest measurement frequency, probably due to more relevant network analyzer calibration errors. Similar results have been obtained for the other matrix coefficients, for a number of different devices, and for different bias conditions.

It can be concluded that the scaling rules evaluated for different K are substantially equivalent; therefore, the choice of a single active slice per gate finger still represents a rea-

---

[3]The admittance formulation can easily be obtained by applying well-known transformation formulas to the scattering matrix $\underline{\beta}_{\mathbf{AS}}$.

[4]*em*, Sonnet Software Inc., Liverpool, NY.

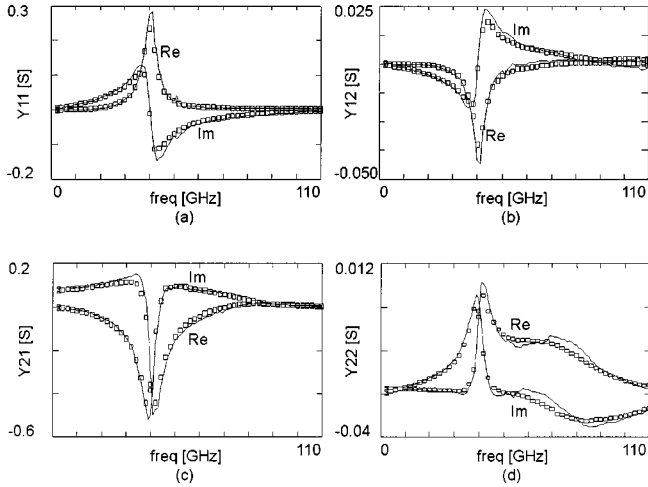[5]The parameter C_{21} has been multiplied by the corresponding number of cells to allow a direct comparison.

Fig. 2. Measured (symbols) and predicted through scaling (lines) Y-parameters for a PML 6×30 μm GaAs pHEMT biased at $Id = Idss$, $Vds = 3$ V. (a) $Y11$. (b) $Y12$. (c) $Y21$. (d) $Y22$.
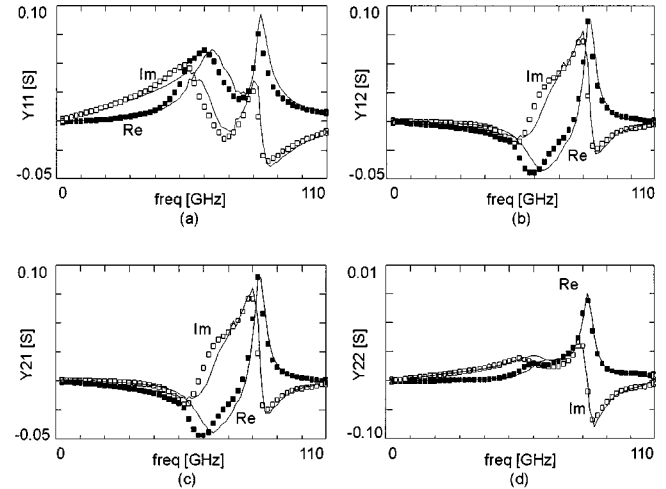

Fig. 4. Measured (symbols) and predicted through scaling (lines) Y-parameters for a PML 2×30 μm GaAs pHEMT biased at $Vgs = -1$ V, $Vds = 3$ V. (a) $Y11$. (b) $Y12$. (c) $Y21$. (d) $Y22$.

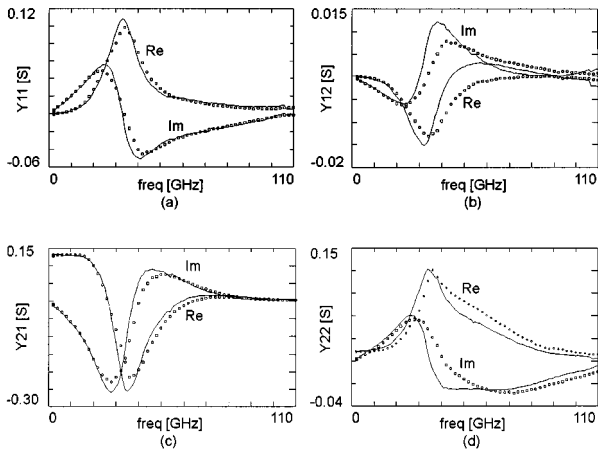Fig. 3. Measured (symbols) and predicted through scaling (lines) Y-parameters for a PML 4×75 μm GaAs pHEMT biased at $Id = Idss$, $Vds = 3$ V. (a) $Y11$. (b) $Y12$. (c) $Y21$. (d) $Y22$.
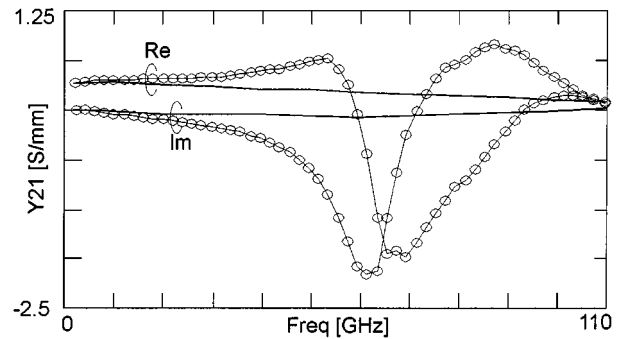

Fig. 5. Measured admittance $Y21$ per unit of gatewidth (symbols) for a PML 2×30 μm GaAs pHEMT biased at $Id = Idss$, $Vds = 3$ V. Continuous lines represent the corresponding extracted admittance parameter $Y_{AS,21}$ of the internal elementary devices.

sonable choice (giving also a good tradeoff between accuracy and complexity) for the modeling of FET devices also at millimeter-wave frequencies. For this reason, the experimental results in the following are provided for the case $K = 1$.

In order to test the actual predictive capabilities and physical consistency of the proposed scaling approach up to millimeter-wave frequencies, the distributed model was adopted to predict the small-signal performance of several 0.2-μm Philips Microwave Limeil (PML) GaAs pHEMTs [29], having a different number of gate fingers and gatewidths. In particular, the scaling functions in (6) were identified starting from the 2×15 μm, 2×60 μm, 2×120 μm, and 4×30 μm devices and then used to predict the performance of devices having different geometries. For instance, Figs. 2 and 3 show the comparison between the measured admittance parameters and the corresponding predicted values for a 6×30 μm and 4×75 μm device in the bias point $Vds = 3$ V and $Vgs = 0$ V, while in Fig. 4, the same comparison for a 2×30 μm device is reported for the almost pinched-off condition $Vds = 3$ V and $Vgs = -1$ V. The reasonably good agreement confirms

the robustness and consistency of the proposed approach up to millimeter-wave frequencies even when a simple linear regression is adopted for model scaling.

IV. FREQUENCY EXTRAPOLATION OF THE MODELING APPROACH

In Fig. 5, the measured admittance parameter Y_{21} (per unit of gatewidth) is shown versus frequency up to 110 GHz for a PML 2×30 μm pHEMT biased at $I_D = I_{DSS}$, $Vds = 3$ V. In this figure, the corresponding extracted admittance parameter $Y_{AS,21}$ of the internal elementary devices, obtained considering a single active slice per finger, is also drawn. It is possible to observe the resonant-like behavior of the measured admittance parameter in comparison with the quite regular, smooth, and almost linear shape of the internal elementary device admittance. Very similar results are also obtained for the other admittance matrix elements and for a great variety of bias conditions. This is not surprising since extrinsic parasitic effects cause very often such a kind of resonance in most devices observed in the Y-domain, while the regular frequency behavior of the internal active slice admittance is consistent with physical hypothesis of short memory conditions, which usually hold for
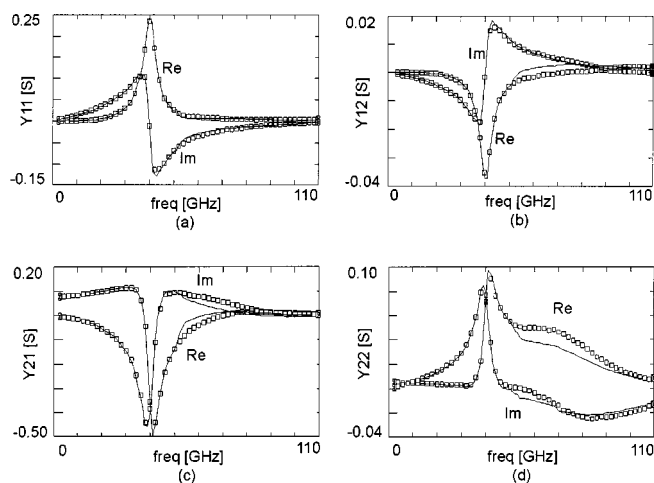
Fig. 6. Measured (symbols) and predicted through frequency extrapolation above 50-GHz (lines) admittance parameters for a PML 6 × 30 μm GaAs pHEMT at $Id = Idss$, $Vds = 3$ V. (a) $Y11$. (b) $Y12$. (c) $Y21$. (d) $Y22$.

Fig. 8. Measured (symbols) and predicted through frequency extrapolation above 50-GHz (lines) admittance parameters for a PML 4 × 30 μm GaAs-pHEMT at $Vgs = -1$ V, $Vds = 3$ V. (a) $Y11$. (b) $Y12$. (c) $Y21$. (d) $Y22$.
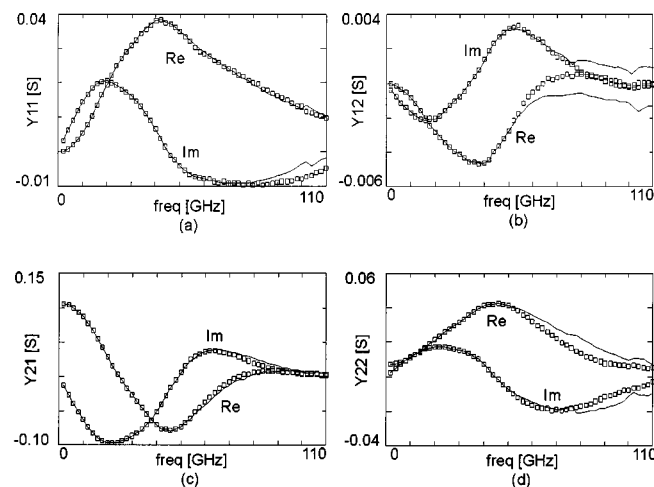

Fig. 7. Measured (symbols) and predicted through frequency extrapolation above 50-GHz (lines) admittance parameters for a PML 2 × 120 μm GaAs pHEMT at $Id = Idss$, $Vds = 3$ V. (a) $Y11$. (b) $Y12$. (c) $Y21$. (d) $Y22$.

the "intrinsic part" of microwave and millimeter-wave devices [30]–[34]. Thus, direct frequency extrapolation of measured device scattering or admittance parameters would lead to very inaccurate prediction results. On the contrary, the almost linear behavior of the internal elementary device admittance suggests an alternative way in performing reliable frequency extrapolation. In fact, these internal admittance coefficients can be suitably approximated and extrapolated by means of low-order polynomial expressions, easily identifiable on the basis of least-square minimization algorithms in the frequency range used in device characterization [35]. Moreover, the frequency-extrapolated polynomial expression of the internal elementary devices can be used in conjunction with the distributed description of the extrinsic passive structure in order to predict the small-signal device behavior at frequencies higher than those used in the identification measurements. To this aim, electromagnetic simulations must be obviously performed up to the highest frequency of interest.
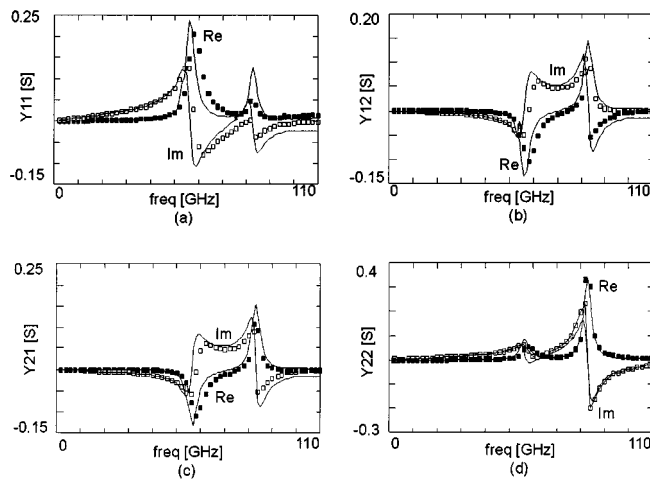
The proposed frequency extrapolation procedure has been experimentally verified using Philips pHEMT devices. In particular, the Y-parameters of devices having different geometry, directly measured on wafer up to 110 GHz by using an HP8510XF network analyzer, were compared with the corresponding predictions obtained by means of the procedure above outlined. In order to achieve these results, the scattering matrix of the extrinsic device passive structure was "initially" computed on a suitable grid of frequencies up to 50 GHz. To this aim, an electromagnetic simulation was performed on the basis of foundry-provided parameters and device GDSII files [29], using the planar 3-D *em* Sonnet electromagnetic simulator (submicrometer grid and quadruple precision were adopted for better accuracy). The active slice matrix $\underline{\mathbf{Y}}_{\mathbf{AS}}(\omega)$ extracted on the basis of 50-GHz S-parameter measurements was then extrapolated up to 110 GHz through a simple linear regression. Finally, the obtained active slice models were connected with the extrinsic passive device structure characterized by means of an "extended" electromagnetic simulation up to 110 GHz. The small-signal predictions presented in this paper were obtained with the proposed model after implementation within the Agilent ADS CAD tool[6] for microwave circuit design.

Extensive experimental validation was performed. In the following, only the results for three pHEMT geometries (i.e., 6 × 30 μm, 2 × 120 μm, and 4 × 30 μm) will be shown in order to confirm the validity of the proposed approach. Figs. 6 and 7 show the comparison between measured and simulated results with frequency extrapolation for two of the devices under test biased at $V_{\mathrm{DS}} = 3$ V and $I_D = I_{\mathrm{DSS}}$. As can be clearly seen, the model allows for reasonably accurate prediction of the dynamic linear device behavior at millimeter-wave frequencies. It is important to observe that the model is capable of predicting resonant-like effects totally occurring in the extrapolated frequency range, as happens in the situation of Fig. 8, where the Y-parameters are reported for the PML

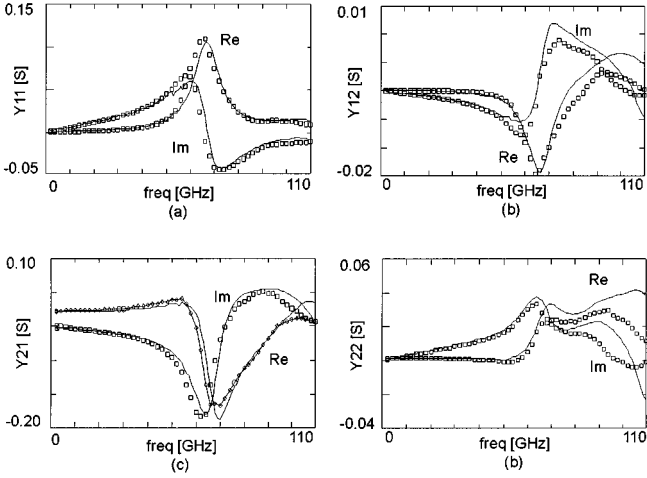[6]ADS, Agilent EEsof EDA release 1.3, Palo Alto, CA 2000.

Fig. 9. Measured (symbols) and predicted through scaling and frequency extrapolation above 50-GHz (lines) admittance parameters for a PML 2×30 μm GaAs-pHEMT at $Id = Idss$, $Vds = 3$ V.

4×30 μm device biased in an almost pinched-off operating condition ($V_{DS} = 3$ V and $V_{GS} = -1$ V).

The presented experimental results clearly exhibit the robustness of the proposed distributed modeling approach and confirm the validity of its physical assumptions. The prediction of the sharp resonant-like device behavior in the Y-domain is, in fact, a difficult task even when occurring in the characterization frequency range, due to the high sensitivity to model errors. Thus, the ability to reproduce the resonance also in the extrapolation frequency region can only relay on the "physical" correctness in combining the accurate electromagnetic simulation results with the almost physically consistent linear approximation/extrapolation of the internal elementary device models.

Finally, both the model features above discussed, i.e., the ability to be correctly *scaled and frequency-extrapolated*, were combined in a final validation test: the *scaled* active slice model of the PML 2×30 μm pHEMT in the 50-GHz frequency range, obtained following the procedure discussed in Section III, was *extrapolated* up to 110 GHz. Fig. 9 shows the corresponding comparison with experimental data confirming that reasonable accuracy is still achievable.

V. CONCLUSION

An empirical scalable distributed approach to the modeling of FETs has been tested up to millimeter waves for devices having a different number of fingers and gatewidths. The model has also been used to accurately predict small-signal device performance up to 110 GHz for Philips 0.2-μm pHEMT devices on the basis of scattering parameters measured up to only 50 GHz. The proposed frequency extrapolation method takes advantage from the physically expected fairly smooth behavior of the admittance parameters of a suitably defined internal elementary device, which can be easily extrapolated by means of low-order polynomials. The model features provide very useful information for circuit designers and for electron device engineers, as they can foresee circuit/device performance with arbitrary electrode metallization of the devices. Moreover, the introduced methodology allows for an accurate characterization

of very high-frequency devices by means of relatively low-cost measurement test sets.

The proposed modeling approach may represent the starting point for the identification of a nonlinear FET model and for the extension of the proposed approach to nonlinear MMIC analysis based on electromagnetic simulation [20]. To this end, mathematical black-box approaches such as those proposed in [30]–[34] can be adopted quite easily. Otherwise, it is obviously possible to use a suitable nonlinear equivalent-circuit structure to model the active slices [36]. Future work will be devoted to this subject.

APPENDIX

Here, the formulation of the system of equations to be solved for model identification as a function of the intrinsic scattering matrix $\underline{\beta}_{AS}$ for values of $K = 2, 3, 4$ are given.

In the case $K = 2$, the problem to be solved assumes the form of a nonlinear system of equation in terms of $\underline{\beta}_{AS}$ as follows:

$$\left(\underline{\beta}_{AS} - \underline{n}_{1,1}\right) \underline{n}_{2,1}^{-1} \left(\underline{\beta}_{AS} - \underline{n}_{2,2}\right) = \underline{n}_{1,2}. \quad (A1)$$

For the case $K = 3$, the problem assumes the following form:

$$\left(\underline{n}_{1,2} - \left[\underline{n}_{1,1} - \underline{\beta}_{AS}\right] \underline{n}_{2,1}^{-1} \left[\underline{\nu}_{2,2} - \underline{\beta}_{AS}\right]\right)$$
$$\cdot \left(\underline{n}_{3,2} - \underline{n}_{3,1} \underline{n}_{2,1}^{-1} \left[\underline{n}_{2,2} - \underline{\beta}_{AS}\right]\right)^{-1}$$
$$- \left(\underline{n}_{1,3} - \left[\underline{n}_{1,1} - \underline{\beta}_{AS}\right] \underline{n}_{2,1}^{-1} \underline{n}_{2,3}\right)$$
$$\cdot \left(\left[\underline{n}_{3,3} - \underline{\beta}_{AS}\right] - \underline{n}_{3,1} \underline{n}_{2,1}^{-1} \underline{n}_{2,3}\right)^{-1} = \underline{0}. \quad (A2)$$

Finally, in the case of $K = 4$, we have

$$\left[\left[\mathbf{T}_6 + \underline{\beta}_{AS}\mathbf{T}_7\right] \mathbf{T}_{16} \left[\mathbf{T}_8 + \mathbf{T}_9\underline{\beta}_{AS}\right]\right]$$
$$\cdot \left[\mathbf{T}_{12} + \mathbf{T}_{13}\underline{\beta}_{AS} - \left[\mathbf{T}_{15} - \underline{\beta}_{AS}\right]\right.$$
$$\left. \cdot \mathbf{T}_{16} \left[\mathbf{T}_8 + \mathbf{T}_9\underline{\beta}_{AS}\right]\right]^{-1}$$
$$+ \left[\left[\mathbf{T}_1 + \mathbf{T}_2\underline{\beta}_{AS} + \underline{\beta}_{AS}\mathbf{T}_3 - \underline{\beta}_{AS}\mathbf{T}_{10}\underline{\beta}_{AS}\right]\right]$$
$$\cdot \left[\mathbf{T}_{12} + \mathbf{T}_{13}\underline{\beta}_{AS} - \left[\mathbf{T}_{15} - \underline{\beta}_{AS}\right]\right.$$
$$\left. \cdot \mathbf{T}_{16} \left[\mathbf{T}_8 + \mathbf{T}_9\underline{\beta}_{AS}\right]\right]^{-1}$$
$$+ \left[\left[\mathbf{T}_6 + \underline{\beta}_{AS}\mathbf{T}_7\right] \mathbf{T}_{16} \left[\mathbf{T}_{11} - \underline{\beta}_{AS}\right]\right.$$
$$\left. - \left[\mathbf{T}_4 + \underline{\beta}_{AS}\mathbf{T}_5\right]\right]$$
$$\cdot \left[\mathbf{T}_{14} - \left[\mathbf{T}_{15} - \underline{\beta}_{AS}\right] \mathbf{T}_{16} \left[\mathbf{T}_{11} - \underline{\beta}_{AS}\right]\right]^{-1} = \underline{0}$$
$$(A3)$$

where

$$\underline{\mathbf{T}}_1 = \underline{\mathbf{n}}_{1,2} - \underline{\mathbf{n}}_{1,1}\underline{\mathbf{n}}_{2,1}^{-1}\underline{\mathbf{n}}_{2,2}$$

$$\underline{\mathbf{T}}_2 = \underline{\mathbf{n}}_{1,1}\underline{\mathbf{n}}_{2,1}^{-1}$$

$$\underline{\mathbf{T}}_3 = \underline{\mathbf{n}}_{2,1}^{-1}\underline{\mathbf{n}}_{2,2}$$

$$\underline{\mathbf{T}}_4 = \underline{\mathbf{n}}_{1,3} - \underline{\mathbf{n}}_{1,1}\underline{\mathbf{n}}_{2,1}^{-1}\underline{\mathbf{n}}_{2,3}$$

$$\underline{\mathbf{T}}_5 = \underline{\mathbf{n}}_{2,1}^{-1}\underline{\mathbf{n}}_{2,3}$$

$$\underline{\mathbf{T}}_6 = \underline{\mathbf{n}}_{1,4} - \underline{\mathbf{n}}_{1,1}\underline{\mathbf{n}}_{2,1}^{-1}\underline{\mathbf{n}}_{2,4}$$

$$\underline{\mathbf{T}}_7 = \underline{\mathbf{n}}_{2,1}^{-1}\underline{\mathbf{n}}_{2,4}$$

$$\underline{\mathbf{T}}_8 = \underline{\mathbf{n}}_{2,1}^{-1}$$

$$\underline{\mathbf{T}}_9 = \underline{\mathbf{n}}_{3,2} - \underline{\mathbf{n}}_{3,1}\underline{\mathbf{n}}_{2,1}^{-1}\underline{\mathbf{n}}_{2,2}$$

$$\underline{\mathbf{T}}_{10} = \underline{\mathbf{n}}_{3,1}\underline{\mathbf{n}}_{2,1}^{-1}$$

$$\underline{\mathbf{T}}_{11} = \underline{\mathbf{n}}_{3,3} - \underline{\mathbf{n}}_{3,1}\underline{\mathbf{n}}_{2,1}^{-1}\underline{\mathbf{n}}_{2,3}$$

$$\underline{\mathbf{T}}_{12} = \underline{\mathbf{n}}_{4,2} - \underline{\mathbf{n}}_{4,1}\underline{\mathbf{n}}_{2,1}^{-1}\underline{\mathbf{n}}_{2,2}$$

$$\underline{\mathbf{T}}_{13} = \underline{\mathbf{n}}_{4,1}\underline{\mathbf{n}}_{2,1}^{-1}$$

$$\underline{\mathbf{T}}_{14} = \underline{\mathbf{n}}_{4,3} - \underline{\mathbf{n}}_{4,1}\underline{\mathbf{n}}_{2,1}^{-1}\underline{\mathbf{n}}_{2,3}$$

$$\underline{\mathbf{T}}_{15} = \underline{\mathbf{n}}_{4,4} - \underline{\mathbf{n}}_{4,1}\underline{\mathbf{n}}_{2,1}^{-1}\underline{\mathbf{n}}_{2,4}$$

$$\underline{\mathbf{T}}_{16} = \left[\underline{\mathbf{n}}_{3,4} - \underline{\mathbf{n}}_{3,1}\underline{\mathbf{n}}_{2,1}^{-1}\underline{\mathbf{n}}_{2,4}\right]^{-1}. \tag{A4}$$

In conclusion, model identification, for $K > 1$ consists of the solution of (A1)–(A3), respectively, for the cases $K = 2, 3, 4$. This task can be accomplished by using one of the widely available routines for the solution of nonlinear systems [37].

ACKNOWLEDGMENT

REFERENCES

[1] J. R. Forrest, "Communication networks for the new millennium," *IEEE Trans. Microwave Theory Tech.*, vol. 47, pp. 2195–2201, Dec. 1999.

[2] W. Heinrich, "On the limits of FET modeling by lumped elements," *Electron. Lett.*, vol. 22, pp. 630–632, 1986.

[3] M. Hammadi and S. El-Ghazaly, "Air-bridged MESFET: A new structure to reduce wave propagation effect in high-frequency transistors," *IEEE Trans. Microwave Theory Tech.*, vol. 47, pp. 890–899, June 1999.

[4] T. Shibata and E. Sano, "Characterization of MIS structure coplanar transmission lines for investigation of signal propagation in integration in integrated circuits," *IEEE Trans. Microwave Theory Tech.*, vol. 38, pp. 881–890, July 1999.

[5] M. Piket-May, A. Taflove, and J. Baron, "FD-TD modeling of digital signal propagation in 3-D circuits with passive and active loads," *IEEE Trans. Microwave Theory Tech.*, vol. 42, pp. 1514–1523, Aug. 1994.

[6] K. C. Gupta, "Emerging trends in millimeter-wave CAD," *IEEE Trans. Microwave Theory Tech.*, vol. 46, pp. 747–755, June 1998.

[7] M. A. Alsunaidi, S. M. S. Imtiaz, and S. M. El-Ghazali, "Electromagnetic wave effects on microwave transistors using a full-wave time domain model," *IEEE Trans. Microwave Theory Tech.*, vol. 44, pp. 799–808, June 1996.

[8] R. O. Grondin, S. M. El-Ghazaly, and S. Goodnick, "A review of global modeling of charge transport in semiconductors and full-wave electromagnetics," *IEEE Trans. Microwave Theory Tech.*, vol. 47, pp. 817–830, June 1999.

[9] W. Heinrich and H. L. Hartnagel, "Wave propagation on MESFET electrodes and its influence on transistor gain," *IEEE Trans. Microwave Theory Tech.*, vol. MTT-35, pp. 1–8, May 1987.

[10] A. Cidronali, "Behavioral and physics based models of high frequency FETs," Dept. Electron. Telecommun., Ph.D. dissertation, Univ. Florence, Florence, Italy, June 1998.

[11] W. Heinrich, "Full wave analysis of conductor losses on MMIC transmission lines," *IEEE Trans. Microwave Theory Tech.*, vol. 38, pp. 1468–1472, Oct. 1990.

[12] F. Alessandri *et al.*, "Propagation characteristics of lossy distributed GaAs FET structures," in *IEEE MTT-S Int. Microwave Symp. Dig.*, Albuquerque, NM, 1992, pp. 963–966.

[13] K. P. Ma, M. Chen, B. Houshmand, Y. Qian, and T. Itho, "Global time-domain full-wave analysis of microwave circuits involving highly nonlinear phenomena and EMC effects," *IEEE Trans. Microwave Theory Tech.*, vol. 47, pp. 859–866, June 1999.

[14] M. B. Steer *et al.*, "Global modeling of spatially distributed microwave and millimeter-wave systems," *IEEE Trans. Microwave Theory Tech.*, vol. 47, pp. 830–839, June 1999.

[15] M. A. Alsunaidi, S. M. S. Imitaz, and S. M. El-Ghazaly, "Electromagnetic wave effects on microwave transistors using a full-wave time-domain model," *IEEE Trans. Microwave Theory Tech.*, pp. 799–808, June 1996.

[16] S. M. S. Imitaz and S. M. El-Ghazaly, "Global modeling of millimeter-wave circuits: Electromagnetic simulation of amplifiers," *IEEE Trans. Microwave Theory Tech.*, vol. 45, pp. 2208–2216, Dec. 1997.

[17] S. Goasguen and S. M. S. El-Ghazaly, "A practical large-signal global modeling simulation of a microwave amplifier using artificial neural network," *IEEE Microwave Guided Wave Lett.*, vol. 10, pp. 273–275, July 2000.

[18] P. Ciampolini, L. Roselli, G. Stopponi, and R. Sorrentino, "Global modeling strategies for the analysis of high-frequency integrated circuits," *IEEE Trans. Microwave Theory and Tech.*, vol. 47, pp. 950–955, June 1999.

[19] E. Larique *et al.*, "Linear and nonlinear FET modeling applying an electromagnetic and electrical hybrid software," *IEEE Trans. Microwave Theory and Tech.*, vol. 47, pp. 915–918, June 1999.

[20] A. Cidronali, G. Collodi, G. Vannini, A. Santarelli, and G. Manes, "A new approach to FET model scaling and MMIC design based on electromagnetic analysis," *IEEE Trans. Microwave Theory and Tech.*, vol. 47, pp. 900–907, June 1999.

[21] R. H. Jansen and P. Pogatzki, "Nonlinear distributed modeling of multifinger FETs/HEMT's in terms of layout-geometry and process-data," in *Proc. 21st Eur. Microwave Conf.*, Stuttgart, Germany, 1991, pp. 609–614.

[22] R. Hajji and F. M. Ghannouchi, "Small signal distributed model for GaAs HBT's and S-parameter prediction at millimeter-wave frequencies," *IEEE Trans. Electron Devices*, vol. 44, pp. 723–732, May 1997.

[23] J. P. Mondal, "Distributed scaling approach of MESFET's and its comparison with lumped-element approach," *IEEE Trans. Microwave Theory Tech.*, vol. 37, pp. 1085–1090, July 1989.

[24] T. M. Martin-Guerrero and C. Camacho-Penalosa, "Nonlinearities in a MESFET distributed model," *Int. J. Microwave Millimeter-Wave Computer-Aided Eng.*, vol. 6, no. 4, pp. 243–248, 1996.

[25] B. Castillo, T. Martin-Gurrero, and C. Camacho-Penalosa, "Scalable distributed model for microwave and millimeter-wave monolithic FET-type devices," in *5th Eur. Gallium Arsenide Related III–V Compounds Applicat. Symp.*, Bologna, Italy, Sept. 1997, pp. 135–138.

[26] R. Hajji and F. M. Ghannouchi, "Small signal distributed model for GaAs HBT's and S-parameter prediction at millimeter-wave frequencies," *IEEE Trans. Electron Devices*, vol. 44, pp. 723–732, May 1997.

[27] M. Rudolph, R. Doerner, K. Beilenhoff, and P. Heymann, "Scalable GaInP/GaAs HBT large-signal model," in *IEEE MTT-S Int. Microwave Symp. Dig.*, vol. 2, Boston, MA, June 11–16, 2000, pp. 753–756.

[28] J. Wood and D. E. Root, "Bias-dependent linear scalable millimeter-wave FET model," in *IEEE MTT-S Int. Microwave Symp. Dig.*, vol. 3, Boston, MA, June 11–16, 2000, pp. 1381–1384.

[29] *Foundry Process ED02AH V 1.1 Design Manual*, Philips Microwave, Limeil, France, 1997.

[30] F. Filicori, A. Santarelli, P. Traverso, and G. Vannini, "Electron device model based on nonlinear discrete convolution for large-signal circuit analysis using commercial CAD packages," in *Proc. GAAS'99*.

[31] F. Filicori, G. Vannini, and V. A. Monaco, "A nonlinear integral model of electron devices for HB circuit analysis," *IEEE Trans. Microwave Theory Tech.*, vol. 40, pp. 1456–1464, July 1992.

[32] F. Filicori, G. Vannini, A. Santarelli, A. Mediavilla, A. Tazon, and Y. Newport, "Empirical modeling of low-frequency dispersive effects due to traps and thermal phenomena in III–V FET's," *IEEE Trans. Microwave Theory Tech.*, vol. 43, pp. 2973–2981, Dec. 1995.

[33] G. Vannini, F. Filicori, and A. Santarelli, "Integral approaches to nonlinear modeling of electron devices," presented at the IEEE MTT-S Nonlinear Meas. Modeling Workshop, Denver, CO, 1997.

[34] F. Filicori, G. Vannini, and A. Santarelli, "A finite-memory nonlinear model for microwave electron devices," in *Proc. 27th Eur. Microwave Conf.*, Sept. 1997.

[35] A. Cidronali, G. Collodi, G. Vannini, and A. Santarelli, "110 GHz scalable FET model based on 50 GHz S-parameter measurements," in *IEEE MTT-S Int. Microwave Symp. Dig.*, Boston, MA, June 2000, pp. 11–16.

[36] R. H. Jansen and P. Pogatzki, "Nonlinear distributed modeling of multifinger FETs/HEMT's in terms of layout-geometry and process-data," in *Proc. 21st Eur. Microwave Conf.*, Stuttgart, Germany, 1991, pp. 609–614.

[37] W. H. Press, B. P. Flannery, S. A. Teykolsky, and W. T. Vetterling, *Numerical Recipes in C: The Art of Scientific Computing*. Cambridge, U.K.: Cambridge Univ. Press, 1998, pp. 383–389 and 656–666.

Alessandro Cidronali (M'89) was born in Florence, Italy, in 1965. He received the Laurea degree and the Ph.D degree in electronic engineering from the University of Florence, Florence, Italy, in 1992 and 1998, respectively.

In 1993, he joined the Department of Electronics Engineering, University of Florence, where he became a Research Associate in 1999. During his academic career, he has been a Lecturer in courses on applied electronics and solid-state electronics and currently teaches microwave electronics. He is currently involved on basic research on quantum functional devices and their applications to microwave circuits. His research activities cover the study of active and passive compact structures for MMICs, the design of multifunction MMICs for low-power wireless applications, CAD and numerical modeling of GaAs MESFETs, and high electron-mobility transistor (HEMT) electronic devices.

Giovanni Collodi (M'99) was born in Florence, Italy. He received the Electronic Engineering degree in 1996.

Following graduation, he joined the Microelectronic Laboratory, Department of Electronics and Telecommunications, University of Florence, where he is involved in the field of MMIC and MMMIC application. His main interests concern the characterization and modeling of devices for MMMIC and MMIC application, which include circuit design.

Alberto Santarelli (M'96) was born in Ferrara, Italy, in 1965. He received the Laurea degree in electronic engineering and the Ph.D. degree in electronics and computer science from the University of Bologna, Bologna, Italy, in 1991 and 1997, respectively.

In 1997, he joined the Research Center for Computer Science and Telecommunication Systems, National Research Council (CSITE-CNR), and in 2000, he became a Research Associate with the Department of Electronics, Computer Science and Systems (DEIS), University of Bologna. During his academic career, he has been a Lecturer in courses on applied electronics and electronics for telecommunications. His main interests are in the fields of nonlinear modeling of microwave devices and circuit design techniques for nonlinear microwave applications.

Giorgio Vannini (S'87–M'92) was born in Città di Castello, Perugia, Italy, in 1960. He received the Laurea degree in electronic engineering and the Ph.D. degree in electronic and computer science engineering from the University of Bologna, Bologna, Italy, in 1986 and 1992, respectively.

In 1992, he became a Research Associate with the Dipartimento di Elettronica, Informatica e Sistemistica (DEIS), University of Bologna. Since 1994, he has also been with the Research Center for Computer Science and Telecommunication Systems, National Research Council–National Research Council (CSITE-CNR), Bologna, Italy, where he is responsible for the MMIC testing and CAD laboratory. Since 1998, he has been an Associate Professor on the Faculty of Engineering, Dipartimento di Ingegneria, University of Ferrara, Ferrara, Italy. During his academic career, he has taught courses in applied electronics, electronics for telecommunications, and industrial electronics. His research activity is mainly devoted to electron device modeling, CAD techniques for MMICs, and nonlinear analysis and design.

Gianfranco Manes (M'01) was born in Florence, Italy, on November 16, 1944.

In 1980, he became an Associate Professor and a Full Professor in 1985. Since the early stages of his career, he has contributed to the field of surface acoustic wave (SAW) technology for RADAR signal processing and electronics countermeasure applications. His major contributions were in introducing novel FIR synthesis techniques, fast analog spectrum analysis configurations, and frequency-hoping waveform synthesis. Since the early 1980s, he has been active in the field of microwave modeling and design. In the early 1990s, he founded and is currently leading the Microelectronics Laboratory, University of Florence, Florence, Italy, which is committed to research in the field of microwave devices. In 1982, he was committed to a buildup of a facility for the design and production of SAW and MIC/MMIC devices, as a subsidiary of a Florence Radar Company, SMA Spa. In 1984, the facility became a standalone privately-owned microwave company, Micrel SpA, operating in the field of defense electronics and space communications. From 1996 to 2000, he was involved in IV framework projects, in the field of information technology applied to the cultural heritage and was invited to orientation meetings and advisory panels for the Commission. His current research interest is in the field of RITD devices for microwave applications in a scientific collaboration with the group at the Physical Science Research Laboratories, Motorola Corporation, Tempe, AZ. He is founder and is currently the President of MIDRA, a research consortium between the University of Florence and the Motorola Corporation. He is the Director of the Italian Ph.D. School in Electronics. In November 2000, he became the Deputy Rector for the Information System of the University of Florence. He has authored over 100 scientific papers in society journals and international conferences.

Dr. Manes is a member of the Board of Italian Electronics Society.